

Submarine groundwater discharge: A large, previously unrecognized source of dissolved iron to the South Atlantic Ocean

Herbert L. Windom^{a,*}, Willard S. Moore^b,
L. Felipe H. Niencheski^c, Richard A. Jahnke^a

^a Skidaway Institute of Oceanography, 10 Ocean Science Circle, Savannah, GA 31411, USA

^b Department of Geological Sciences, University of South Carolina, Columbia, SC 29208, USA

^c Department of Chemistry, Fundação Universidade Federal do Rio Grande, Brazil

Received 9 January 2006; received in revised form 23 June 2006; accepted 26 June 2006

Available online 9 August 2006

Abstract

This paper reports the initial results of a study of groundwater and coastal waters of southern Brazil adjacent to a 240 km barrier spit separating the Patos Lagoon, the largest coastal lagoon in South America, from the South Atlantic Ocean. The objective of this research is to assess the chemical alteration of freshwater and freshwater–seawater mixtures advecting through coastal permeable sands, and the influence of the submarine discharge of these fluids (SGD) on the chemistry of coastal waters. Here we focus on dissolved iron in this system and use radium isotopic tracers to quantify SGD and cross-shelf fluxes. Iron concentrations in groundwaters vary between 0.6 and 180 μM . The influence of the submarine discharge of these fluids into the surf zone produces dissolved Fe concentrations as high as several micromolar in coastal surface waters. The offshore gradient of dissolved Fe, coupled with results for Ra isotopes, is used to quantify the SGD flux of dissolved Fe from this coastline. We estimate the SGD flux to be $2 \times 10^6 \text{ mol day}^{-1}$ and the cross-shelf flux to be $3.2 \times 10^5 \text{ mol day}^{-1}$. This latter flux is equal to about 10% of the soluble atmospheric Fe flux to the entire South Atlantic Ocean. We speculate on the importance of this previously unrecognized iron input to regional ocean production and on the potential significance of this source to understanding variations in glacial–interglacial ocean production.

© 2006 Elsevier B.V. All rights reserved.

Keywords: South Atlantic; Coastal Brazil; Iron; Submarine groundwater discharge; Radium

1. Introduction

Iron is an essential nutrient for ocean primary productivity (Martin et al., 1994; Coale et al., 1996; Boyd et al., 1999, 2000). Variations in iron flux to the

oceans have been linked to glacial–interglacial changes in atmospheric CO_2 as increased productivity initiated by increases in available iron sequesters CO_2 .

Low iron concentrations in seawater, ranging from $\leq 0.2 \text{ nM}$ in surface waters to $\sim 1 \text{ nM}$ at depth (Liu and Millero, 2002; Johnson et al., 1997), are apparently controlled by the availability of organic complexing ligands (Johnson et al., 1997; Barbeau et al., 2001). Iron concentrations relative to N, P, and Si in upwelled waters are generally insufficient to support complete utilization of macronutrients (Frew et al., 2001), thus

* Corresponding author.

E-mail addresses: herb@skio.peachnet.edu,
herb.windom@skio.usg.edu (H.L. Windom),
moore@mail.geol.sc.edu (W.S. Moore), dqmhidro@furg.br
(L.F.H. Niencheski), rick@skio.peachnet.edu (R.A. Jahnke).

requiring additional iron inputs. Atmospheric dust transport is considered the main source of Fe to the open ocean (Duce and Tindale, 1991; Jickells and

Spokes, 2001); recent papers by Bergquist and Boyle (2006) and Vink and Measures (2001) have focused on the effect of this input on the South Atlantic Fe

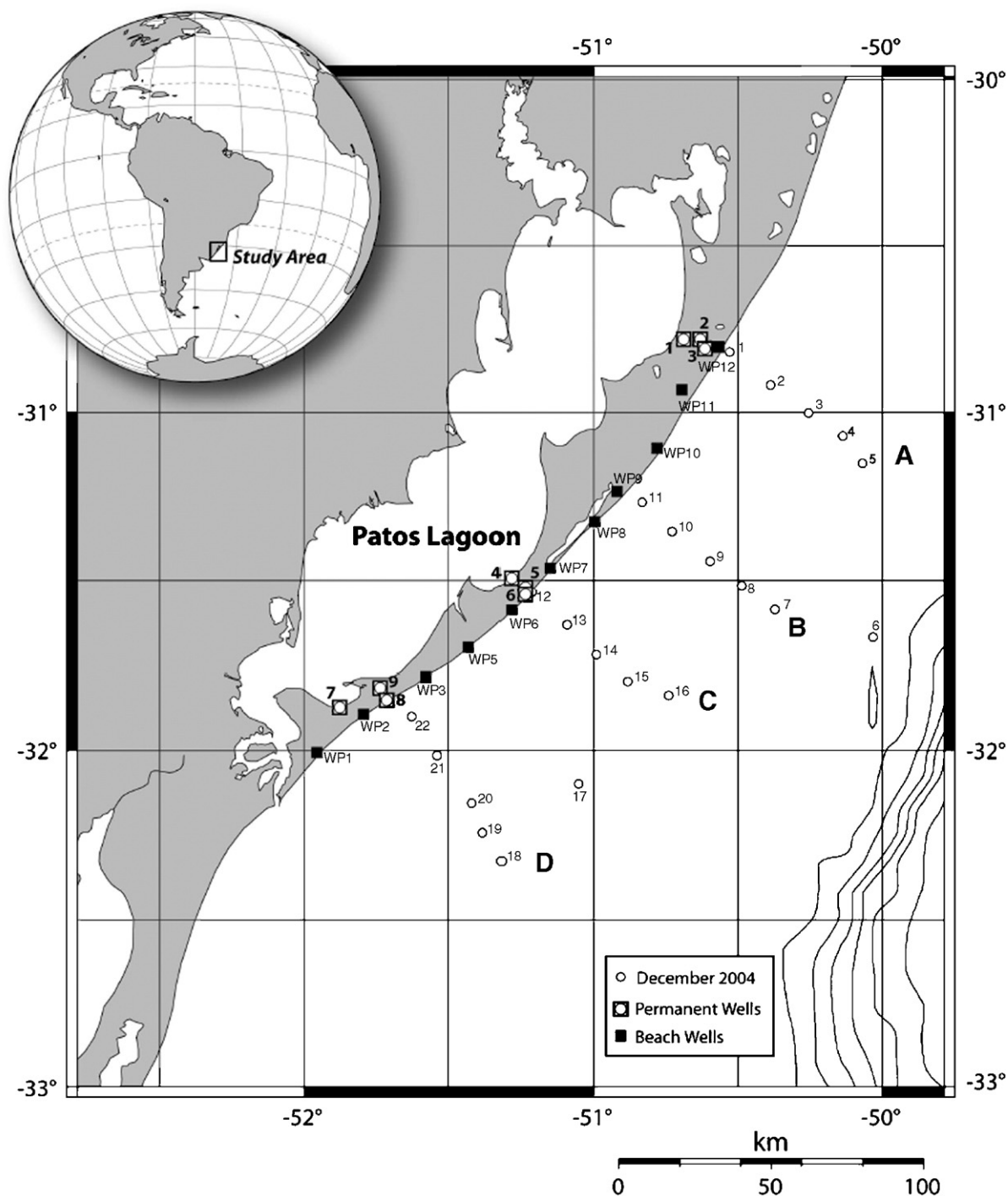


Fig. 1. Patos–Miram Lagoon system. The Miram Lagoon is partially shown in the lower left corner of the figure. Its only outlet to the ocean is through the Patos Lagoon. Map of the study area shows locations of permanent wells, beach groundwater and surf zone stations and offshore hydrographic and water sampling stations. The latter are located along four transect referred to in the text, starting from the north, as Transects, A, B, C and D.

concentrations. Other recognized, but poorly quantified, iron sources to the ocean include rivers and remobilization from sediments (Elrod et al., 2004; Bruland et al., 2005, 2001). Iron in rivers is transported largely in particulate and colloidal forms that are not biologically available. Because these forms are removed rapidly upon mixing with seawater they are considered of only local importance for supporting oceanic marine productivity. Biotic and abiotic processes, however, may mediate the transformation of colloidal and particulate Fe to more available forms, thereby extending the temporal and spatial influence of these sources (Gobler et al., 2002).

An understanding of the marine biogeochemistry of iron, particularly its sources, is clearly important to understanding ocean production and perhaps climate change. But have all of the sources of iron to the ocean been identified and quantified well? Marine geochemists have suspected for some time that submarine groundwater discharge (SGD) provides a significant input of material to the oceans (Garrels and MacKenzie, 1967). SGD, as used in this paper, and previously defined by Burnett et al. (2003), is any and all flow of water on continental margins from the seabed to the coastal ocean, regardless of fluid composition or driving force.

This is consistent with the implied definition used in recent papers where SGD is acknowledged as responsible for important fluxes of some materials to and from the coastal ocean (Bugna et al., 1996; Shaw et al., 1998; Moore, 1996, 1999; Rutkowski et al., 1999; Charette and Sholkovitz, 2006). There is a growing literature on the importance of SGD on coastal ocean chemistry; furthermore, this transport process may also be important to global ocean chemistry. Here we present evidence that SGD is a potential major source of iron to the South Atlantic Ocean.

Our study area is the 240 km-long sandy barrier, formed during the Holocene, separating Patos Lagoon from the South Atlantic Ocean (Fig. 1). Earlier trace element work in Patos Lagoon by Windom et al. (1999), suggested that iron behavior in its freshwater–seawater mixing zone was not controlled by classic two end member mixing and reactions typical of surface estuarine systems (Fig. 2A). Their study was conducted during the summer (December 1995) when freshwater discharge to the lagoon is at a minimum and the salinity gradient (0–30) is spread over 60 nautical miles, mostly within the lagoon. These authors hypothesized that water from Patos Lagoon was mixing with adjacent ocean waters and reacting with sediments within the sandy barrier producing a third end member that mixes

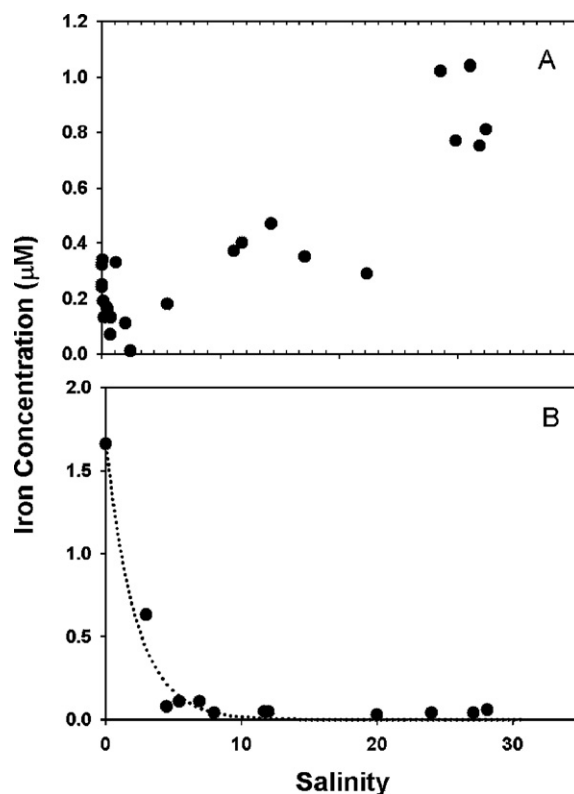


Fig. 2. Dissolved iron vs. salinity in the surface freshwater–seawater mixing zone of the Patos Lagoon during low summer discharge, December 1995 (A) and high winter discharge, June 2001 (B). The high end of the salinity gradient during December 1995 was just out of the mouth of the inlet. During June 2001, the high salinity end of the transect was about 2 km offshore of the mouth.

with surface estuarine waters. Results from a monitoring well drilled on the barrier in June 2001 supported this idea and revealed that the groundwater was chemically very different from both Patos Lagoon and Atlantic Ocean water (Windom and Niencheski, 2003). During June, the winter period, when freshwater discharge was high, results of analyses of surface water samples collected along a transect that extended into the nearshore South Atlantic, revealed an iron mixing behavior typical of most estuarine systems (Fig. 2B). This suggested that during high discharge conditions the influence of the third end member is masked.

Based on these findings, we initiated a research program to assess groundwater–surface water interactions along the coast of the barrier spit enclosing Patos Lagoon and to determine how SGD may influence the biogeochemistry of adjacent shelf and ocean waters in this region. As a part of this research we are studying the behaviour of a suite of trace elements and nutrients as well as radium isotopic tracers. In this paper, however,

our focus is on the importance of the iron source associated with SGD to this region. We use isotopes of radium to assess SGD flux and cross-shelf transport. We also report data on Mn, which has similar geochemical behavior to Fe, and data on Cu, which has dissimilar geochemical behavior.

2. Field and laboratory methods

Field sampling campaigns were conducted during the Austral summer (November 2003 and December 2004) when freshwater discharge to Patos Lagoon is minimal and the salinity of the outflow at its mouth is high (Windom et al., 1999). Data on wind direction and velocity for 1 week prior and the week during our field campaigns were obtained from a meteorological station at the Fundação Universidade Federal do Rio Grande near the mouth of the lagoon. During the November 2003 campaign, mean wind direction was onshore for 4 days with maximum velocities of 6 m s^{-2} , from the south 2 days at less than 2 m s^{-2} , and from the North 9 days at *ca.* 3 m s^{-2} . During the December 2004 campaign, mean wind direction was onshore 4 days at $2\text{--}4 \text{ m s}^{-2}$ and 10 days from the north at $2\text{--}5 \text{ m s}^{-2}$. The Rio de la Plata discharge is also lowest during the Austral summer and the southward along-shore wind stress further minimizes the intrusion of any freshwater from this source into the study area under these conditions (Piola et al., 2005). Some samples of beach groundwater and from the surf zone for metal analyses were collected during the winter (July 2005) when wind stress was variable but more from the south. Even during this period surface salinity measured during a ferry crossing of the lagoon inlet was over 30.

Sampling of the coastal aquifer (i.e. groundwater of the barrier sands) was accomplished by installing PVC, screened permanent wells across three transects of the Patos Lagoon barrier (PLB). Each transect consists of three sets of wells, one near the lagoon, one in the interior and one near the beach front. Each set generally included three wells screened nominally at 5 m, 10 m and 15 m (Fig. 1). We also used a push-point piezometer system to sample groundwater along the beach of the PLB down to a maximum depth of 8 m, but most samples were collected at shallower depths of a meter or two. Sampling sites were spaced at *ca.* 20 km intervals on the southernmost 240 km of the PLB ocean beach. But during July 2005, samples for metal analysis were also collected at locations up to 100 km further north. Water samples from the surf zone were collected at beach sites during all campaigns. Offshore seawater samples were collected in December 2004 along four

transects perpendicular to shore using the fisheries research vessel *Atlantico Sul*. CTD casts were made at each station using a Sea Bird Model 25 Sea Logger.

For radium isotopic analyses, 4–10 L were collected from the permanent wells and the beach piezometers using a peristaltic pump. About 50 L of surf zone water were collected using a clean bucket and 200 L samples of offshore water from 3 to 5 m depth were collected with a submersible pumping system. These samples were immediately processed by passing through manganese oxide coated fibers to retain radium (Moore, 1976). ^{223}Ra and ^{224}Ra in offshore samples were measured immediately after collection and within 3 days for well samples using a delayed-coincidence system as described by Moore and Arnold (1996). Later, radium was leached from the fibers and ^{226}Ra and ^{228}Ra were measured by gamma spectrometry (Moore, 1984).

Samples for trace metal analyses were collected from wells and offshore by two separate peristaltic pumping systems that use a single length of acid cleaned silicone tubing connected directly to disposable cartridge filters. For offshore samples, the intake end of the tubing was fitted with a Teflon vane, which oriented into the current. This was hung on Kevlar rope and deployed at a depth of 5 m or more to be significantly below the keel of the ship. Samples were pumped directly through Aqua Prep 600, $0.45 \mu\text{m}$ cartridge filters after flushing the tubing and the filter with several liters of sample water for permanent well and offshore samples. For surf zone and beach groundwater samples the system was flush with less volume because of filter clogging. In-line filtered samples were collected directly into 500-mL acid precleaned linear polyethylene bottles, after rinsing, acidified with 0.5 mL of ultra pure nitric acid and stored in plastic bags to return to SkIO for analysis. The push-point piezometer system consisted of stainless steel pipe sections through which a Teflon tube was passed and connected to the stainless steel, screened intake end. Samples were collected, as described above, using a peristaltic pumping system whereby samples were filtered as they were collected. Surf zone samples were collected by wading to a depth of about 1 m and using an acid-cleaned 4-L polyethylene bottle after rinsing with ambient water. A 500 mL aliquot of this water was collected as described above, using the peristaltic pumping system connected to the cartridge filters so that samples were pumped and filtered from the collecting bottle within minutes of collection.

A subset of beach groundwater and surf zone samples from the December 2004 campaign was collected into acid-precleaned 50-mL polyethylene

syringes with polypropylene plungers after filtering ($0.45\ \mu\text{m}$) in the field. Each evening about 20 mL of these samples were filtered through $0.02\ \mu\text{m}$ Anotop 25 filters, using the technique of Shiller (2003), and collected into acid-cleaned polyethylene vials and acidified with 10 μL of nitric acid.

We used extraction columns of Toyopearl® AF-Chelate 650 M (Willie et al., 1998) to separate and concentrate trace metal from estuarine and coastal water samples. Iron, Mn, Cu, Co, Cd, V, Zn, are among the metals which we routinely extract along with standards in this way and this approach was used for all offshore samples. Groundwater and surf zone samples were

extracted using the same technique. Because these samples were so high in Fe it was realized quickly that it was more efficient to analyze the unextracted filtered samples diluted 20 to 100 times with ultra pure distilled water.

For most metals we used a VG Plasma Quad II+ ICPMS for analyte quantification. Because isobaric interferences for Fe are encountered with this instrument, we quantified this metal using Zeeman corrected graphite furnace AA (Perkin Elmer AAnalyst 800). We estimate sampling/analytical blanks for groundwater samples as $\leq 10\ \text{nM}$ for Fe and Mn and $<0.1\ \text{nM}$ for Cu based on blank double-distilled water passed through

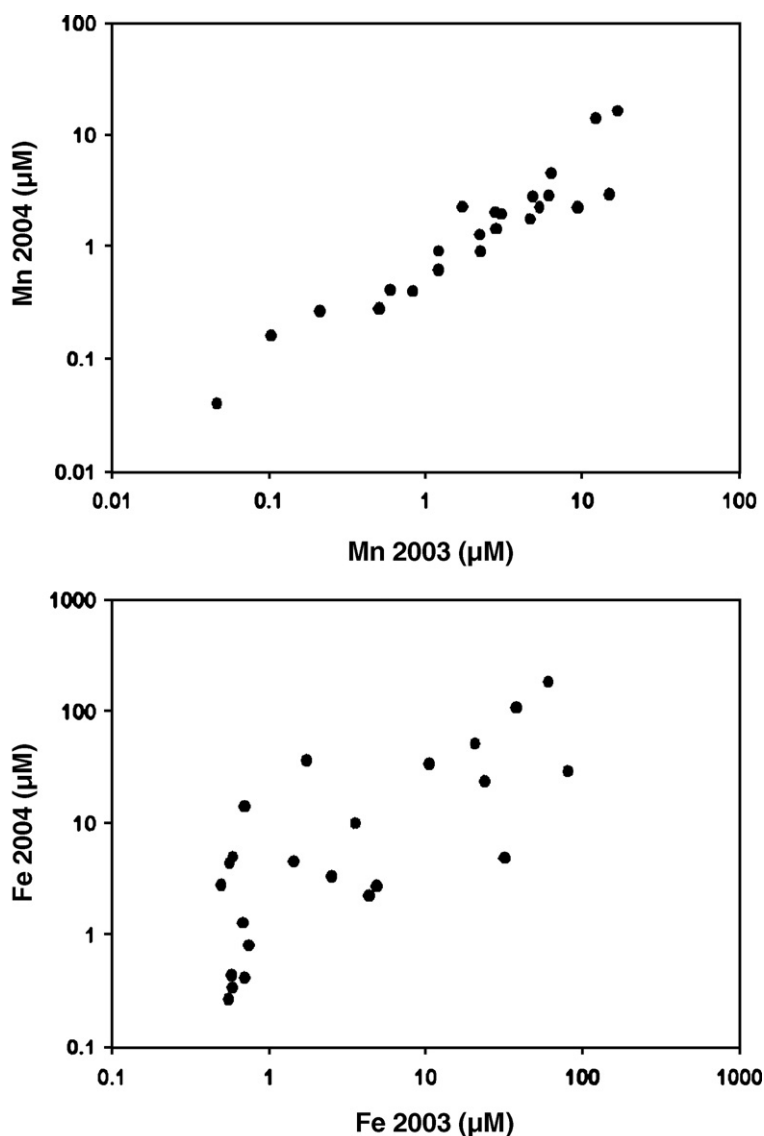


Fig. 3. Dissolved iron and manganese in permanent wells. Results for samples collected during December 2004 are plotted against those collected during November 2003.

the push-point sampling apparatus and filtered through the Aqua Prep filters (directly out of their plastic seals as was done in the field) after flushing with 2 L. For offshore samples this estimate is ≤ 5 nM, ≤ 0.5 nM and ≤ 0.1 nM for Fe, Mn, and Cu, respectively, based on distilled water passed through the peristaltic pumping system and the Aqua Prep filters, and extraction column blanks. These values were used to correct results for these samples. Six replicate analyses of separate samples from the most offshore station (Station 6, Fig. 2) yielded concentrations of 10 ± 4 nM and 1 ± 0.2 nM and 1.5 ± 0.2 nM for Fe, Mn and Cu, respectively.

3. Results

3.1. Permanent wells

Our initial conceptual model of this system assumed that freshwater from the Lagoon advects through the permeable sands of the barrier spit in response to a hydrologic head created by the lagoon. Water levels in the lagoon reach up to 3 m asl as a result of wind stress and runoff, but are always above sea level virtually throughout the Lagoon (Windom and Niencheski, 2003). Once wells were in place, however, it became clear that

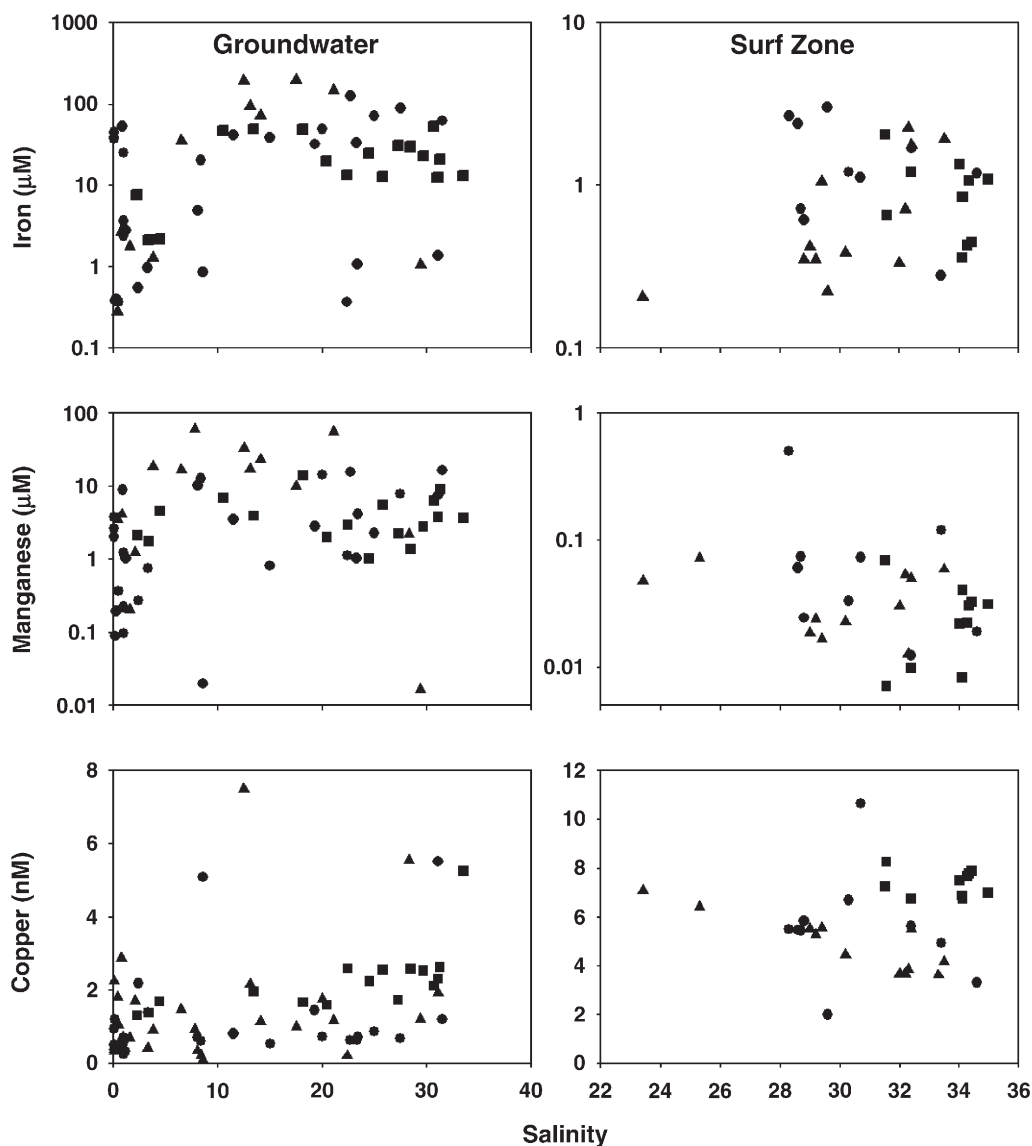


Fig. 4. Concentrations of dissolved Fe, Mn and Cu in beach groundwater and in the surf zone (November 2003 – ●; December 2004 – ■; July 2005 – ▲).

Table 1

Comparison of iron concentrations (μM) in 0.45 μm and 0.02 μm filtrates of surf zone and beach groundwater samples

Distance (km)	Surf zone				Beach groundwater		
	Fe (0.45 μm)	Fe (0.02 μm)	% Passing 0.02 μm	Depth (m)	Fe (0.45 μm)	Fe (0.02 μm)	% Passing 0.02 μm
0				1	48.5	0.9	1.8
60	2.05	1.11	54.1	1	7.6	4.1	53.1
80	0.65	0.61	93.2	1	31.0	9.0	28.9
100	1.21	0.54	44.4	3	2.1	0.9	40.2
100				4	2.2	0.4	18.1
120	1.08	1.51	140.0	1	53.3	18.6	35.0
140	0.45	0.36	80.0	1	12.9	1.7	13.0
140				2	20.8	0.3	1.2
180	0.85	0.68	80.0				
180	0.36	0.36	100.1	1	24.6	21.1	86.1
180				2	19.8	0.7	3.4
200	0.36	0.36	100.1	1	12.6	0.3	2.6
200				2	23.1	0.4	1.9
220	0.43	0.43	100.0	1	13.2	0.3	2.4
220				2	29.7	0.7	2.4
240	1.09	0.29	26.2	1	12.7	0.4	3.1
Average	0.95	0.65	67.7		20.9	4.0	19.0

Distance is northward from mouth of Patos Lagoon.

the system is more complex because some wells near the lagoon flowed with a hydraulic head up to 4 m above the adjacent lagoon water level. Nonetheless, samples from these wells should be representative of freshwater flowing through the barrier spit toward the ocean.

Before collecting water samples for analysis, the wells were pumped to clear the volume of the PVC pipe. Water was pumped through a chamber which contained pH, DO and temperature sensors. For all wells, DO was always around 30 μM but we assume that this is an upper limit because of the chance of aeration during pumping and/or because we were using a Clark Cell DO sensor which has a long equilibration time at low DO. The pH varied from

4.7 to 7.1 with a mean of 6.1. Iron and Mn concentrations showed no relation to pH and ranged from 0.6 to 180 μM and from 0.05 to 17 μM , respectively, similar to the ranges reported for the freshwater region of the subterranean estuary studied by Charette and Sholkovitz (2006). Concentrations, however, did appear to relate to the specific collection site with highest and lowest concentrations occurring in the same wells for samples collected in 2003 and 2004 (Fig. 3). In contrast, copper (data not shown) exhibited a relatively small concentration range of 0.4–4.2 nM normally distributed around *ca.* 1.5 nM. Iron and Mn are clearly controlled by redox conditions, which probably relate to groundwater advection rates and are

Table 2

Samples collected from the surf zone (left) and well points on the adjacent beach (right)

km	Surf zone samples				Beach well point samples			
	Date	Salinity	^{226}Ra	^{228}Ra	Date	Salinity	^{226}Ra	^{228}Ra
20	7-Dec-04	33.52	8.87	20.8	1-Dec-04	18.2	30.9	154.0
40	7-Dec-04	34.00	8.54	24.0				
60	7-Dec-04	35.30	7.68	21.4	1-Dec-04	2.3	7.1	59.2
80	6-Dec-04	32.80	6.16	15.6	1-Dec-04	27.3	25.8	70.1
100	6-Dec-04	32.20	6.55	17.5				
120	6-Dec-04	33.50	5.99	15.0	2-Dec-04	30.7	68.8	255.9
140	6-Dec-04	33.00	6.25	14.9	2-Dec-04	33.5	34.2	126.4
160	6-Dec-04	36.53	7.49	17.6	3-Dec-04	13.4	24.5	159.0
180	6-Dec-04	36.41	7.67	21.4	3-Dec-04	24.5	16.6	81.6
200	6-Dec-04	36.79	6.86	16.8	4-Dec-04	31.1	45.2	142.8
220	6-Dec-04	35.87	7.22	19.6	4-Dec-04	22.4	24.5	55.8
240	6-Dec-04	35.56	7.97	21.1	4-Dec-04	25.8	13.7	40.7
	Average	34.62	7.27	18.8	Average	22.91	29.1	114.6

Distance in km is north of the mouth of Patos Lagoon. Ra activities are dpm/100 L.

thus site specific, whereas Cu is probably controlled by CuS solubility.

3.2. Beach groundwater and surf zone

Groundwater samples collected along the beach (Fig. 1) had a salinity range of 0 to *ca.* 34 with no consistent trend with distance from the mouth of the lagoon. For the 6 profiles for which we collected samples at 1 m intervals to a depth of 4 m or more, salinities were highest in the surface samples for four of the profiles and

more or less uniform in the other two. In most cases, groundwater salinities were always lower than those of the adjacent surf zone.

In beach groundwater samples, iron concentrations had a range similar to that observed for the permanent wells (Fig. 4). Adjacent surf zone concentrations were about an order of magnitude lower. For Mn, concentrations in fresher samples from the groundwater mixing zone had a range similar to that for samples collected from the permanent wells, but at higher salinities, concentrations increased. This again is similar to the

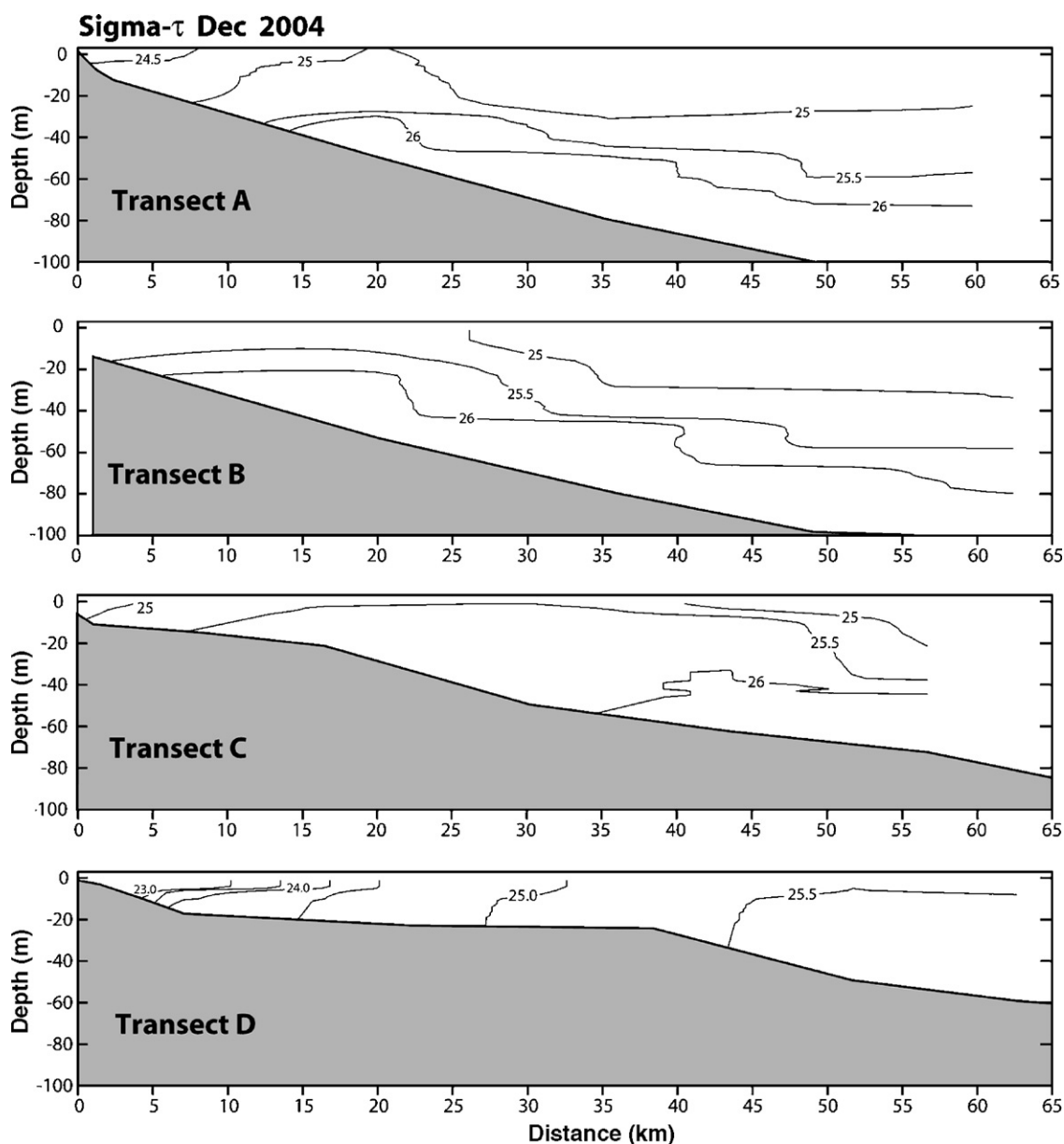


Fig. 5. Sigma- τ contours, based on CTD casts, along the four offshore transects.

results of Charette and Sholkovitz (2006) who found Mn concentrations to reach highest levels in the intermediate salinity region of their subterranean estuary. Manganese concentrations in the surf zone were lower than those in adjacent groundwater by a hundred-fold. The high productivity of the surf zone, results in super saturation of DO and a particle-rich environment favorable for Fe and Mn removal. Almost 70% of the iron in surf zone samples passed a 0.02 μm filter as compared with less than 20% for beach groundwater samples (Table 1).

The distribution of Cu in the groundwater mixing and surf zones is considerably different from Fe and Mn.

Copper concentrations in the low to intermediate salinity groundwater are the same as those of groundwater collected from the permanent wells, but at higher salinities Cu concentrations increase. Concentrations in the surf zone are also increased presumably due to oxidation of copper sulfides. Kinetics of CuS formation are likely slow enough relative to advective transport to allow high dissolved Cu concentrations to occur in the higher salinity region of the groundwater mixing zone.

Radium isotope activities in the beach groundwater averaged 30 and 1200 dpm/100 L for ^{226}Ra and ^{228}Ra , respectively (Table 2).

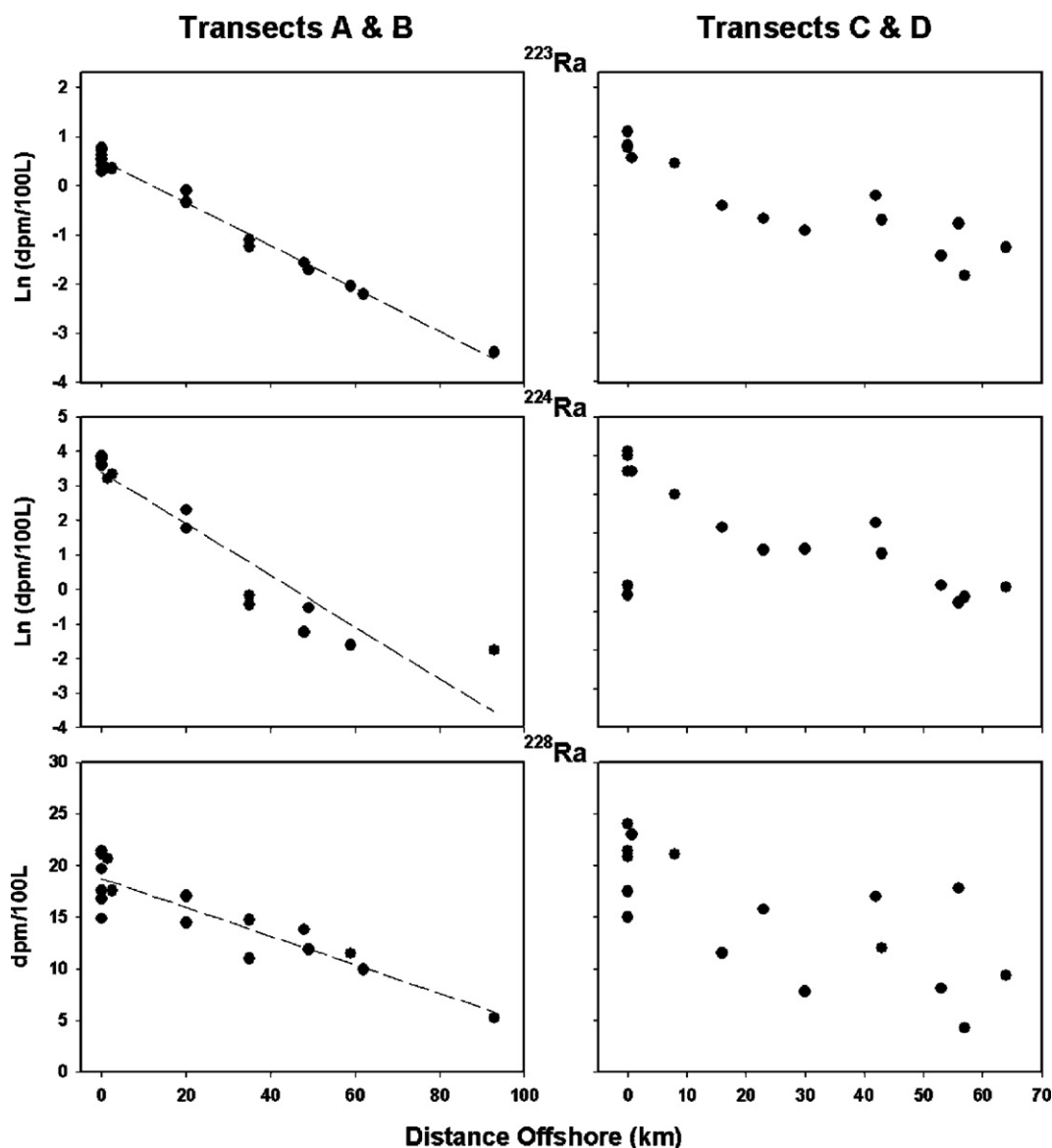


Fig. 6. Variations in cross-shelf concentrations of radium isotopes. For Transects A and B, equations for regression curves are: $\ln^{223}\text{Ra}=0.519-0.043x$ ($r^2=.99$); $\ln^{224}\text{Ra}=3.39-0.075x$ ($r^2=.89$); $^{228}\text{Ra}=18-0.14x$ ($r^2=.82$); $\ln\text{Fe}=5.5-0.043x$ ($r^2=.54$), where x =distance offshore in km.

3.3. Offshore samples

During December 2004 we occupied four 60 km offshore transects and one station (6) 90 km offshore (Fig. 1). Density (σ_t) profiles from the CTD casts (Fig. 5) revealed that the two northern transects (A and B) were stratified with a 10–20 m surface layer separated from bottom waters. Sigma t profiles along the two southern transects (Transects C and D) indicate little stratification of the water column. The lack of stratification means the surface samples from the

southern C and D transects may be influenced by input from the seabed.

3.3.1. Radium isotopes

The surface ^{228}Ra distribution along transects A and B is best described as mixing of an enriched nearshore source and a depleted offshore end member (Fig. 6). The surface ^{228}Ra distribution along transects C and D is irregular. Similar differences are noted for the short-lived isotopes. The surface ^{223}Ra and ^{224}Ra distributions along transects A and B decrease exponentially

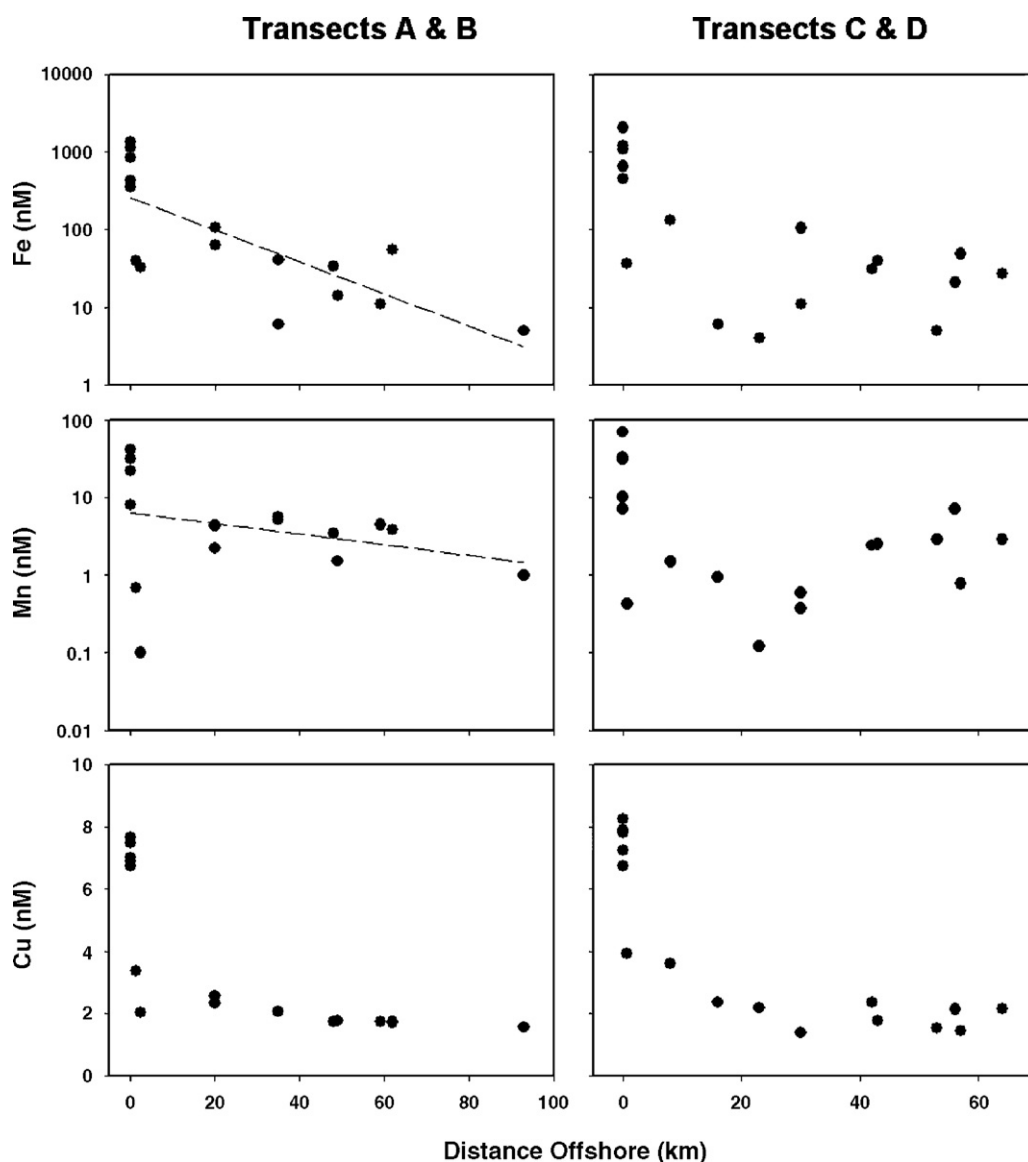


Fig. 7. Cross-shelf variations in dissolved Fe, Mn and Cu. The line shown in the Fe vs. distance plot for Transects A and B is the regression curve which follows the equation: $\ln\text{Fe} = 5.4 - 0.044 \cdot \text{distance}$.

with distance. The distributions of ^{224}Ra and ^{223}Ra along transects C and D are irregular.

3.3.2. Metals

The offshore distributions of Fe, Mn, and Cu follow different patterns (Fig. 7). Fe decreases exponentially toward the open ocean station. Concentrations of Fe in the surf zone averaged 0.9 nM, but dropped sharply just offshore. Mn concentrations decrease abruptly to minimum concentrations within 10 km of shore. The copper data follow the smoothest trend as compared to Fe and Mn, reflecting the relatively small variations in mixing end members (i.e. SGD, coastal, oceanic).

4. Discussion

4.1. SGD

The surf zone samples show no relation between salinity and distance from the mouth of Patos Lagoon, in fact some samples collected furthest from the mouth had the lowest salinities (Table 2). Since there is no other source of fresh surface water, we conclude that SGD from the permeable barrier selectively reduces the ocean salinity along this coastline.

The beach groundwater had extremely high dissolved (0.45 μm filtered) Fe concentrations (2 to 53 μM). This range is not surprising given those reported in coastal groundwater elsewhere (Charette et al., 2005). Although dissolved Fe concentrations were lower in the surf zone by an order of magnitude (0.3–2 μM) compared to groundwater, they were 3–4 orders of magnitude greater than open ocean concentrations, which are less than 1 nM for the South Atlantic (Vink and Measures, 2001; Bergquist and Boyle, 2006). These ocean samples were collected 20–240 km away from the mouth of Patos Lagoon and, like salinity, Fe concentrations showed no relation to distance from the mouth. Also, the wind conditions precluded any significant intrusions of surface runoff into the area from the lagoon inlet or from the Rio de la Plata. Even when conditions might favor iron input from the lagoon (e.g. during high surface runoff in June 2001), our results (Fig. 2B) suggest that Fe concentrations above a salinity of 30 are less than 100 nM in samples affected by this source. We therefore conclude that surface outflow from the lagoon is not the source of elevated Fe in the surf zone of our study area. Instead we hypothesize that SGD is the source. As for the source of Fe to the shelf area, discussed below, one reviewer of this paper suggests that other sources such as sediment

diagenetic processes, sediment resuspension, SGD from shelf sediments, direct runoff from coastal soils, etc., could provide the sources for the observed Fe levels in the coastal ocean. We cannot demonstrate that these processes are not responsible but, nonetheless, believe that the evidence provided below is more consistent with a nearshore SGD of water similar in composition to the beach groundwater.

Our conceptual model of how the SGD Fe flux is maintained is as follows: There is a continual supply of Fe in fresh suboxic groundwater moving toward the coastline driven by local and/or regional hydraulic gradients. The Mercosul aquifer (also known as the Guarani aquifer), which underlies virtually all of southern Brazil, Uruguay, Paraguay and northern Argentina, is one of the largest fresh groundwater systems in the world (Araújo et al., 1999). Araújo et al. argue that most of the flow in this system is to the southwest, toward the Parana basin, and suggest that “negligible discharge” is to the Atlantic; but they provide no data to indicate what that volume might be. While the Patos–Miram Lagoon system certainly provide local hydraulic gradients resulting in groundwater flow toward the South Atlantic along a *ca.* 600 km length of coastline, we speculate that the Mercosul or another more regional aquifer may have an even greater geographic influence and may, in fact, provide for SGD on the shelf.

As the Fe-enriched suboxic groundwater moves toward the ocean it encounters oxygenated seawater forming a relative narrow mixing zone along the shoreline (groundwater from wells located just behind the beach dune are fresh at all depths). This is similar to the subterranean estuary studied by Charette and Sholkovitz (2006). As demonstrated by these authors, much of the Fe probably precipitates at this redox interface. Although we did not collect cores for analysis of solids, we observed numerous patches of iron-rich sands on the beach surface where SGD was evident. We suggest, however, that the dynamic circulation of seawater through the permeable beach sands allows a significant amount of reduced iron to escape into the surf zone with the SGD before being oxidized.

The beach groundwater also contains high activities of ^{228}Ra (40 to 260 dpm/100 L, but only moderate activities of ^{226}Ra (7.1 to 69 dpm/100 L) (Table 2). The surf zone samples are enriched in ^{228}Ra (15 to 21 dpm/100 L) compared to the open ocean (5 dpm/100 L), but only slightly to not at all enriched in ^{226}Ra (6.9 to 8.9 dpm/100 L) compared to the open ocean (7.8 dpm/100 L). Moore (2003) has shown that aquifers that are rapidly flushed with salty water contain much higher

activities of ^{228}Ra than ^{226}Ra . We thus conclude that the surf zone ^{228}Ra enrichments are due to SGD.

4.2. Coastal mixing and SGD flux

To quantify SGD fluxes to the coastal ocean, a measure of the residence time of these waters with respect to mixing with the open ocean is required. The short-lived radium isotopes (^{224}Ra , half-life=3.66 days, and ^{223}Ra , half-life=11.4 days) provide one means of measuring this mixing rate. These isotopes are contributed to nearshore waters by SGD and release from sediments. Once introduced to the water activities decrease by mixing with lower activity water and by radioactive decay. Moore (2000) has demonstrated that the distribution of the short-lived isotopes over the shelf can be modelled to yield mixing rates. The solution of the mixing equation for the short-lived radium isotopes is

$$\ln A_x = \ln A_{x=0} - (\lambda/K_h)^{1/2} x \quad (1)$$

where A_x is the measured activity at distance x , $A_{x=0}$ is the activity at the shoreline, K_h is the mixing coefficient, and λ is the decay constant. Several assumptions are required to use this model: (1) radium addition to the surface water occurs only in the near-shore zone; (2) net cross-shelf advection is zero; (3) cross-shelf mixing is constant; (4) the system is steady state. There was a strong pycnocline across the shelf on transects A and B except within 10 km of shore (Fig. 5). This should prevent radium released into the bottom water on the shelf from reaching the surface. The pycnocline was not present on transects C and D. We conclude that the first assumption is valid for transects A and B, but not for C and D. Along transects A and B, ^{228}Ra decreases linearly across the shelf (Fig. 6). This implies that constant mixing, not advection, controls the distribution and supports the second and third assumptions. Along transects A and B, ^{223}Ra and ^{224}Ra decrease exponentially across the shelf (Fig. 6). This also implies that the mixing rate is constant, and supports the third assumptions. Due to limited ship time, we could not test assumption (4). The slope of the $\ln \text{Ra}$ vs. distance plot is $(\lambda/K_h)^{1/2}$. Solving for K_h yields mixing rates of $338 \text{ m}^2 \text{ s}^{-1}$ and $240 \text{ m}^2 \text{ s}^{-1}$ for ^{223}Ra and ^{224}Ra , respectively. We will use the ^{223}Ra rate because this isotope can be measured with confidence farther offshore, as reflected by the better fit of the data.

At steady state the offshore flux of radium must be balanced by new inputs. The offshore flux of ^{228}Ra is the product of its concentration gradient (Fig. 6, $1.5 \text{ dpm m}^{-3} \text{ km}^{-1}$) and the mixing rate. Using a mixing rate of $338 \text{ m}^2 \text{ s}^{-1}$ and assuming all export is

through a minimal 10-m-deep mixed layer, the offshore flux is $4.4 \times 10^8 \text{ dpm km}^{-1} \text{ day}^{-1}$. If this flux occurs throughout the 240 km study area, the total flux is $1.1 \times 10^{11} \text{ dpm day}^{-1}$. If this flux is sustained by water similar to the beach groundwater samples (average $^{228}\text{Ra}=1230 \text{ dpm m}^{-3}$), the total SGD flux is $8.5 \times 10^7 \text{ m}^3 \text{ day}^{-1}$. Here we neglect SGD that may occur into bottom waters 10–40 km offshore.

4.3. Fe inputs

To estimate the iron flux to nearshore waters, we multiply the ratio of iron to ^{228}Ra in the beach groundwaters ($27.6 \mu\text{mol Fe/dpm Ra}$) by the ^{228}Ra flux, to yield an iron flux of $3 \times 10^6 \text{ mol day}^{-1}$. Alternately, the flux can be estimated by multiplying the average iron concentration in the beach groundwaters ($24 \pm 1 \mu\text{mol L}^{-1}$) by the SGD flux. This yields an iron flux of $2 \times 10^6 \text{ mol day}^{-1}$. We use the smaller estimate and point out much of the Fe in the SGD to the coastal zone is likely removed from solution by a number of processes that either remove it permanently or cycles it back to the groundwater system. Even so, this provides an estimate of the magnitude of the process.

4.4. Fe removal rate and cross-shelf fluxes

The distribution of dissolved Fe across the shelf on transects A and B follows an exponential curve similar to the short-lived Ra isotopes, albeit with more scatter (Fig. 7). We use the slope of this curve to determine the removal rate of dissolved Fe as water mixes across the shelf. In Eq. (1) we substitute k , a first order removal rate, for λ , the decay constant. The slope of the Fe curve in Fig. 7 is $(k/K_h)^{1/2} = 0.044 \text{ km}^{-1}$. Using $K_h = 338 \text{ m}^2 \text{ s}^{-1}$, we calculate $k = 0.03 \text{ day}^{-1}$. Thus, Fe is removed from solution with a half-life of 23 days. We point out that this is based on the regression curve through the data which also contains the surf zone where Fe averaged about $1 \mu\text{M}$. The intercept of the regression curve is about 500 nM which suggests that much of the removal occurs near shore.

To estimate how much iron crosses the shelf we need the average concentration of iron and the residence time of water. We define the residence time of water on the shelf as the time required to remove the water from $1/e$ of the width of the shelf (22 km) and use the relationship

$$L = (2K_h t)^{1/2} \quad (2)$$

where L is length (22 km), K_h is mixing rate ($338 \text{ m}^2 \text{ s}^{-1}$), and t is residence time. Thus the residence

time is 8.3 days. The average iron concentration in the inner 22 km (excluding the surf zone samples) is 50 nM, the volume is 5.3×10^{13} L ($22 \text{ km} \times 240 \text{ km} \times 10 \text{ m}$), so 3.2×10^5 mol of iron must be exported across the shelf every day. This implies a dissolved Fe flux that is significantly less than the SGD estimated for the nearshore suggesting that *ca.* 90% is removed from solution in the inner shelf zone. Alternatively, a larger amount of the SGD Fe flux could have been removed in the nearshore followed by additional iron inputs from other sources as mentioned in Section 4.1 above. The dissolved Fe export is nevertheless quite large. The fate of particulate Fe that should be associated with this transport is unknown.

The significance of these fluxes becomes apparent when compared to other potential sources of Fe to the South Atlantic. The Parana River, which accounts for 90% of the Rio de la Plata, has an average discharge of $14,000 \text{ m}^3 \text{ s}^{-1}$ and if its Fe concentration is near the world riverine average of $1 \mu\text{M}$ (Martin and Meybeck, 1979), the flux is $\sim 1.2 \times 10^6 \text{ mol day}^{-1}$, or about half the Fe SGD flux to our study area. The cross-shelf riverine flux must be much smaller as 90% or more of the riverine supply is likely removed during estuarine mixing similar to what we observed in our early studies in the mixing zone of the Patos Lagoon (Fig. 2). An estimate of the dissolved atmospheric Fe flux of $8 \times 10^{10} \text{ g year}^{-1}$ (Duce and Tindale, 1991) to the entire South Atlantic Ocean is *ca.* $3.8 \times 10^6 \text{ mol day}^{-1}$. Our conservative estimate of the cross-shelf Fe flux from a 240-km coastline is *ca.* 10% of this, clearly demonstrating the likely importance of the SGD source.

The potential significance of the Fe flux from permeable sediments to regional ocean primary production is not only due to its magnitude, but also to the penetration of the iron offshore. The decrease of Fe in the mixed layer across the shelf (Fig. 7, transects A and B) has a scale length (i.e. $1/\text{slope}$) of 23 km, which is similar to the 16 km scale length for the penetration of iron from coastal California into the North Pacific (Johnson et al., 1997; Elrod et al., 2004) and to the 0.17 km scale length for the offshore iron decrease from the Peruvian shelf (Bruland et al., 2005). But, the initial concentration for our study region is ~ 1000 times greater than those for the California or Peruvian shelves. This difference is likely due to the combination of processes that control iron release to the study area. For example, the Fe input to the Peruvian shelf, where concentrations greater than 50 nM are observed in bottom waters, is apparently due to the flux from anaerobic, organic-rich, muddy sediments (Bruland et al., 2005). For our study area the Fe flux is from

permeable sands and is associated with a dense diatom bloom of *Asterionellopsis glacialis* in the surf zone. Such blooms are common along this coast and in other coastal areas (Brezinski, 1985; Odebrecht et al., 1995). There is abundant literature on the ability of diatoms, bacteria and other marine microorganisms to produce Fe-complexing ligands, which maximize Fe availability in time and space (Frew et al., 2001; Gobler et al., 2002). The fact that almost 70% of the iron in surf zone samples passed a $0.02 \mu\text{m}$ filter as compared with less than 20% for beach groundwater samples (Table 1), suggests that the nearshore biological production may mediate the formation of smaller, presumably more labile or colloidal, species of Fe. This would allow Fe to penetrate further into the ocean, where it could be entrained in the Brazil Current and transported south to support production in the nutrient-rich waters of the Brazil/Malvinas Confluence and the upwelling along the continental shelf break (Fig. 8). Iron fertilization experiments in the Southern Ocean (Bowie et al., 2001) have demonstrated that while added iron is rapidly taken up by surface plankton, it is efficiently recycled and can remain in surface waters, supporting higher biomass, for at least 40 days. This observation is qualitatively consistent with our measurements and implies that iron from SGD could persist in surface waters long enough to be transported large distances from shore. We speculate that the flux of iron from SGD through

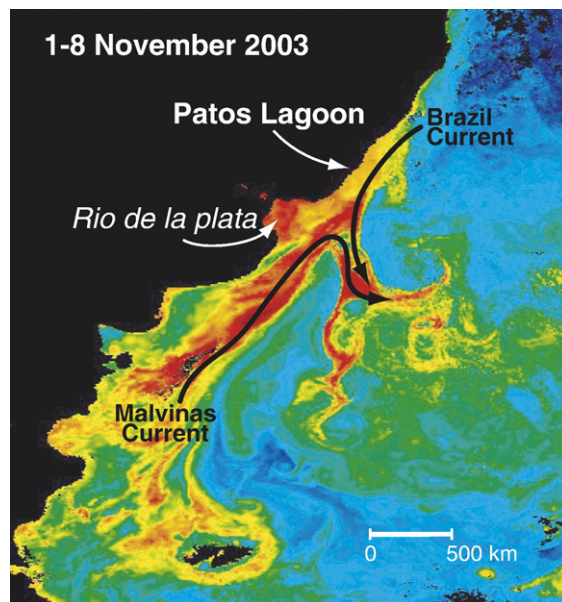


Fig. 8. MODIS ocean color image showing chlorophyll along the frontal zone of the Brazil–Malvinas Confluence. Image provided by the SeaWiFS Project, NASA/Goddard Space Flight Center and ORBIMAGE. Distance scale is approximate.

permeable sediments, which may extend over 600 km of coastline in this area, could be the most significant iron source in the region and may be essential for the high regional productivity.

4.5. Implications of the Fe flux

The identification of this previously unrecognised source of Fe to the South Atlantic may have additional important global implications. The linkages among iron input, dust input, ocean productivity, and climate change in the southern ocean have been a major driver of oceanic and paleoceanographic research since the “Iron Hypothesis” was first suggested by John Martin (1990). A recent compilation of paleoceanographic studies (Gall et al., 2001) from which biological productivity variations between glacial and interglacial periods could be estimated, suggests that most proxies of productivity south of the polar front decreased or at least did not increase during the last glacial maximum despite increases in dust deposition as recorded in Antarctic ice cores. These results suggest that the dust iron hypothesis can not fully explain glacial–interglacial atmospheric $p\text{CO}_2$ variations and seems contradictory to the observed stimulation of production by iron addition (Kohfeld et al., 2005). However, an expected correlation between dust and ocean productivity assumes that dust is the dominant source of iron to surface waters. Elrod et al. (2004) and Bruland et al. (2005) have demonstrated the importance of ocean margins as iron sources to the ocean. Our results are consistent with these findings, although the mechanisms differ. If these findings can be generalized and ocean margins are major sources of iron to the oceans during interglacial periods, the apparent contradiction may be reconciled if SGD Fe sources decrease during glacial times. We suggest that future studies must examine the global extent of ocean margin iron sources and the role of SGD as a transport mechanism to assess the variability of this input in the context of paleoceanographic reconstructions and climate change.

Acknowledgements

The authors wish to thank Debbie Wells, Mary Richards and Julie Amft for their assistance in field sampling and analyses. We also thank the students and staff of FURG and the captain and crew of *R/V Atlantico Sul*. We also express thanks to the three anonymous reviewers of this paper who provided many helpful comments. This work was supported in part by the National Science Foundation (OCE-0233465, HLW and

RAJ, OCE-0233657, WSM) and CNPq (Brazil – Grants 490126/2003-0 and 301219/2003-6).

References

- Araújo, L.M., França, A.B., Potter, P.E., 1999. Hydrogeology of the Mercosul aquifer system in the Paraná basin, South America, and comparison with the Navajo–Nugget aquifer system, USA. *Hydrogeol. J.* 7, 317–336.
- Barbeau, K., Rue, E.L., Bruland, K.W., Butler, A., 2001. Photochemical cycling of iron in the surface ocean mediated by microbial iron(III)-binding ligands. *Nature* 413, 409–413.
- Bergquist, B.A., Boyle, E.A., 2006. Dissolved iron in the tropical and subtropical Atlantic Ocean. *Glob. Biogeochem. Cycles* 20, GB1015. doi:10.1029/2005GB002505.
- Bowie, A.R., Maldonado, M.T., Frew, R.D., Croot, P.L., Achterberg, E.P., Mantoura, R.F.C., Worsfold, P.J., Law, C.S., Boyd, P.W., 2001. The fate of added iron during a mesoscale fertilization experiment in the Southern Ocean. *Deep-Sea Res.* II 48, 2703–2743.
- Boyd, P.W., LaRoche, J., Gall, M., Frew, R., McKay, R.M.L., 1999. The role of iron, light, and silicate in controlling algal biomass in sub-Antarctic waters SE of New Zealand. *J. Geophys. Res.* 104, 13395–13408.
- Boyd, P., Watson, A.J., Law, C.S., Ts Trull, E.R.A., Murdoch, R., Bakker, D.C.E., Bowie, A.R., Buesseler, K.O., Chang, H., Charette, M., Croot, P., Downing, K., Frew, R., Gall, M., Hadfield, M., Hall, J., Harvey, M., Jameson, G., LaRoche, J., Liddicoat, M., Ling, R., Maldonado, M.T., McKay, R.M., Nodder, S., Pickmere, S., Pridmore, R., Rintoul, S., Safi, K., Sutton, P., Strzepek, R., Tanneberger, K., Turner, S., Waite, A., Zeldis, J., 2000. A mesoscale phytoplankton bloom in the polar Southern Ocean stimulated by iron fertilization. *Nature* 407, 695–702.
- Brezinski, M.A., 1985. The Si:C:N ratio of marine diatoms: interspecific variability and the effect of some environmental variables. *J. Phycol.* 21, 347–357.
- Bruland, K.W., Rue, E.L., Smith, G.J., 2001. Iron and macronutrients in California coastal upwelling regimes: implication for diatom blooms. *Limnol. Oceanogr.* 46, 1661–1674.
- Bruland, K.W., Rue, E.L., Smith, G.J., DiTullio, G.R., 2005. Iron, macronutrients and diatom blooms in the Peru upwelling regime: brown and blue waters of Peru. *Mar. Chem.* 93, 81–103.
- Bugna, G.C., Chanton, J.P., Young, J.E., Burnett, W.C., Cable, P.H., 1996. The importance of groundwater discharge to the methane budgets of nearshore and continental shelf waters of the northeastern Gulf of Mexico. *Geochim. Cosmochim. Acta* 60 (23), 4735–4746.
- Burnett, W.C., Bokuniewicz, H., Huettel, M., Moore, W.S., Taniguchi, M., 2003. Groundwater and pore water inputs to the coastal zone. *Biogeochemistry* 66, 3–33.
- Charette, M.A., Sholkovitz, E.R., 2006. Trace element cycling in a subterranean estuary: Part 2. Geochemistry of the pore water. *Geochim. Cosmochim. Acta* 70 (4), 811–826.
- Charette, M.A., Sholkovitz, E.R., Hansel, C.M., 2005. Trace element cycling in a subterranean estuary: Part 1. Geochemistry of permeable sediments. *Geochim. Cosmochim. Acta* 69, 2095–2109.
- Coale, K.H., Johnson, K.S., Fitzwater, S.E., Gordon, R.M., Tanner, S., Chavez, F.P., Ferioli, L., Sakamoto, C., Rogers, P., Millero, F., Steinberg, P., Nightingale, P., Cooper, D., Cochlan, W.P., Landry, M.R., Constantinou, J., Rollwagen, G., Trasvina, A., Kudela, R., 1996. A massive phytoplankton bloom induced by an ecosystem-

- scale fertilization experiment in the equatorial Pacific Ocean. *Nature* 383, 495–501.
- Duce, R.A., Tindale, N.W., 1991. Atmospheric transport of iron and its deposition in the ocean. *Limnol. Oceanogr.* 36, 1715–1726.
- Elrod, V.A., Berelson, W.M., Coale, K.H., Johnson, K.S., 2004. The flux of iron from continental shelf sediments; a missing source for global budgets. *Geophys. Res. Lett.* 31, L12307. doi:10.1029/2004GL020216.
- Frew, R., Bowie, A., Croot, P., Pickmere, S., 2001. Macronutrient and trace-metal geochemistry of an in situ iron-induced Southern Ocean bloom. *Deep-Sea Res.*, II 48, 2467–2481.
- Gall, M.P., Strzepek, R., Maldonado, M., Boyd, P.W., 2001. Phytoplankton processes: Part 2. Rates of primary production and factors controlling algal growth during the Southern Ocean Iron Release Experiment (SOIREE). *Deep-Sea Res.*, II 48, 2571–2590.
- Garrels, R.M., MacKenzie, F.T., 1967. *Evolution of Sedimentary Rocks*. Norton and Co.
- Gobler, C.J., Donat, J.R., Consolvo III, J.A., Sañudo-Wilhelmy, S.A., 2002. Physiochemical speciation of iron during coastal algal blooms. *Mar. Chem.* 77, 71–89.
- Jickells, T.D., Spokes, L.J., 2001. Atmospheric Fe inputs to the oceans. In: Tuner, D.R., Hunter, K. (Eds.), *The Biogeochemistry of Fe in Seawater*. John Wiley and Sons Ltd., Chichester, pp. 85–121.
- Johnson, K.S., Gordon, R.M., Coale, K.H., 1997. What controls dissolved iron concentrations in the world ocean? *Mar. Chem.* 57, 137–161.
- Kohfeld, K.E., Le Quere, C., Harrison, S.P., Anderson, R.F., 2005. Role of marine biology in glacial–interglacial CO₂ cycles. *Science* 308, 74–78.
- Liu, X., Millero, F.J., 2002. The solubility of iron in seawater. *Mar. Chem.* 77, 43–54.
- Martin, J.H., 1990. Glacial–interglacial CO₂ change: the iron hypothesis. *Paleoceanography* 5, 1–14.
- Martin, J.M., Meybeck, M., 1979. Elemental mass-balance of material carried by world major rivers. *Mar. Chem.* 7, 173–206.
- Martin, J.H., Coale, K.H., Johnson, K.S., Fitzwater, S.E., Gordon, R.M., Tanner, S.J., Hunter, C.N., Elrod, V.A., Nowicki, J.L., Coley, T.L., Barber, R.T., Lindley, S., Watson, A.J., Van Scoy, K., Law, C.S., Liddicoat, M.I., Ling, R., Stanton, T., Stockel, J., Collins, C., Anderson, A., Bidigare, R., Ondrusek, M., Latasa, M., Millero, F.J., Lee, K., Yao, W., Zhang, J.Z., Friederich, G., Sakamoto, C., Chavez, F., Buck, K., Kolber, Z., Greene, R., Falkowski, P., Chisholm, S.W., Hoge, F., Swift, R., Yungel, J., Turner, S., Nightingale, P., Hattton, A., Liss, P., Tindale, N.W., 1994. Testing the iron hypothesis in ecosystems of the equatorial Pacific Ocean. *Nature* 371, 123–129.
- Moore, W.S., 1976. Sampling radium-228 in the deep ocean. *Deep-Sea Res.* 23, 647–651.
- Moore, W.S., 1984. Radium isotope measurements using germanium detectors. *Nucl. Instrum. Methods* 223, 407–411.
- Moore, W.S., 1996. Large groundwater inputs to coastal waters revealed by ²²⁶Ra enrichments. *Nature* 380, 612–614.
- Moore, W.S., 1999. The subterranean estuary: a reaction zone of ground water and sea water. *Mar. Chem.* 65, 111–126.
- Moore, W.S., 2000. Determining coastal mixing rates using radium isotopes. *Cont. Shelf Res.* 20, 1993–2007.
- Moore, W.S., 2003. Sources and fluxes of submarine discharge delineated by radium isotopes. *Biogeochemistry* 66, 75–93.
- Moore, W.S., Arnold, R., 1996. Measurement of ²³³Ra and ²²⁴Ra in coastal waters using a delayed coincidence counter. *J. Geophys. Res.* 101, 1321–1329.
- Odebrecht, C., Segatto, A.Z., Freitas, C.A., 1995. Surf-zone chlorophyll *a* variability at Cassino Beach, Southern Brazil. *Estuar. Coast. Shelf Sci.* 41, 81–90.
- Piola, A.R., Matano, R.P., Palma, E.D., Möller Jr., O.O., Campos, E.J.D., 2005. The influence of the Plata River discharge on the western South Atlantic shelf. *Geophys. Res. Lett.* 32, LXXXXX. doi:10.1029/2004GL021638.
- Rutkowski, C.M., Burnett, W.C., Iverson, R.L., Chanton, J.P., 1999. The effect of groundwater seepage on nutrient delivery and seagrass distribution in the northeastern Gulf of Mexico. *Estuaries* 22 (4), 1033–1040.
- Shaw, T.J., Moore, W.S., Kloepper, J., Sochaski, M.A., 1998. The flux of barium to the coastal waters of the southeastern United States: the importance of submarine groundwater discharge. *Geochim. Cosmochim. Acta* 62 (18), 3047–3054.
- Shiller, A.M., 2003. Syringe filtration methods for examining dissolved and colloidal trace elements in remote field locations. *Environ. Sci. Technol.* 37, 3953–3957.
- Vink, S., Measures, C.I., 2001. The role of dust deposition in determining surface water distributions of Al and Fe in the south west Atlantic. *Deep-Sea Res.*, Part II 48, 2787–2809.
- Willie, S.N., Iida, Y., McLaren, J.W., 1998. Determination of Cu, Ni, Zn, Mn, Co, Pb, Cd, and V in seawater using flow injection ICP-MS. *At. Spectr.* 19, 67–72.
- Windom, H., Niencheski, F., 2003. Biogeochemistry in a freshwater–seawater mixing zone in permeable sediments along the coast of Southern Brazil. *Mar. Chem.* 83, 121–130.
- Windom, H.L., Niencheski, L.F., Smith Jr., R.G., 1999. Biogeochemistry of nutrients and trace metals in the estuarine region of the Patos Lagoon (Brazil). *Estuar. Coast. Shelf Sci.* 48, 113–123.